Cutin-Derived Oligomers Act as Damage-Associated Molecular Patterns in *Arabidopsis thaliana*

Carlos J.S. Moreira[a], Rita Escórcio[a], Artur Bento[a], Marta Bjornson[b,f], Ana S. Tomé[a], Celso Martins[a,g], Mathieu Fanuel[c,d], Isabel Martins[a], Benedicte Bakan[d], Cyril Zipfel[b,e*] and Cristina Silva Pereira[a,*]

[a]Instituto de Tecnologia Química e Biológica António Xavier, Universidade Nova de Lisboa, Oeiras, Portugal.

[b]Institute of Plant and Microbial Biology, Zurich-Basel Plant Science Center, University of Zurich, Zurich, Switzerland.

[c]PROBE research infrastructure, BIBS Facility, INRAE, Nantes, France.

[d]Research Unit Biopolymers Interaction Assemblies, INRAE, Nantes, France.

[e]The Sainsbury Laboratory, University of East Anglia, Norwich Research Park, Norwich, United Kingdom.

[f]Present address: Department of Sciences, University of California, Davis, USA.

[g]Present address: Center for Integrative Genomics, Faculty of Biology and Medicine, University of Lausanne, Lausanne, Switzerland.

[*]Corresponding authors: Cyril Zipfel (cyril.zipfel@botinst.uzh.ch) and Cristina Silva Pereira (spereira@itqb.unl.pt)

Abstract

The cuticle constitutes the outermost defensive barrier of most land plants. It comprises a polymeric matrix – cutin, surrounded by soluble waxes. Moreover, the cuticle constitutes the first line of defense against pathogen invasion, while also protecting the plant from many abiotic stresses. Aliphatic monomers in cutin have been suggested to act as immune elicitors in plants. This study analyses the potential of tomato cutin oligomers to act as damage-associated molecular patterns (DAMPs) able to induce a rapid immune response in the model plant *Arabidopsis*. Cutin oligomeric mixtures led to Ca^{2+} influx and MAPK activation in *Arabidopsis*. Comparable responses were measured for cutin, which was also able to induce a reactive oxygen species (ROS) burst. Furthermore, treatment of *Arabidopsis* with cutin oligomers resulted in a unique

transcriptional reprogramming profile, having many archetypal features of pattern-triggered immunity (PTI). Targeted spectroscopic and spectrometric analyses of the cutin oligomers suggest that the elicitors compounds consist mostly of two up to three 10,16-dihydroxyhexadecanoic acid monomers linked together through ester bonds. This study demonstrates that cutin breakdown products can act as DAMPs; a novel class of elicitors deserving further characterization.

Introduction

Plants occupied land environments approximately 450 million years ago (Delwiche and Cooper, 2015). The transition from water to land habitats exposed plants to numerous challenges imposed by an extremely desiccating environment (Waters, 2003). To control water loss, protect against UV radiation and pathogens, and reinforce the epidermal cell layer, plants developed a hydrophobic barrier – the cuticle (Martin and Rose, 2014; Fich et al., 2016). The cuticle is composed of a polymeric matrix of cutin to which organic solvent soluble lipids (waxes) associate (Yeats and Rose, 2013). In addition, cutin interaction with the polysaccharides that build up the epidermal cell walls has been proposed (Philippe et al., 2020a; Xin and Fry, 2021), but the nature of such anchoring remains uncertain.

During infection of the aerial organs of plants, fungal spores release cutin-degrading enzymes – cutinases, having esterase activity (Longhi and Cambillau, 1999) that can disrupt the polymeric matrix and release cutin-derived molecules. Perception of these molecules by the fungus increases the production of cutinases that breach the cuticle barrier, thus allowing the fungus to invade the plant organ (Kolattukudy et al., 1995).

To fend off pathogen invasion, plants have developed a highly specialized mechanism to sense biotic threats by using cell surface pattern recognition receptors (PRRs)(Zipfel, 2014). These receptors perceive pathogen-associated molecular patterns (PAMPs) and damage-associated molecular patterns (DAMPs), derived from the invading pathogens or from the breakdown of plant tissues, respectively (Zipfel, 2014). Cutin aliphatic monomers (*i.e.* the major basic elements composing the cutin polymer) have been proposed as DAMPs due to their ability to induce some elements of a canonical immune

response, namely the production of reactive oxygen species (ROS) in cucumber, rice and *Arabidopsis thaliana* (hereafter *Arabidopsis*), and the upregulation of defense-related genes in rice and *Arabidopsis* (Kauss et al., 1999; Kim et al., 2008; Park et al., 2008). Exogenous application of monomers obtained from plants having augmented cuticular permeability (*SlSHN3*-OE), increased the resistance of Micro-Tom tomato plants against the fungal pathogen *Botrytis cinerea*, and activated defense responsive genes (Buxdorf et al., 2014); however, the nature of the elicitor(s) remains unresolved. Cutin aliphatic monomers were also reported to induce the production of antimicrobial compounds (Serrano et al., 2014). Although cutin monomers have been proposed as DAMPs, their capabilities to elicit other important hallmark early immune responses, for example intracellular calcium influx and activation of mitogen-activated protein kinases (MAPKs), have never been observed (Serrano et al., 2014; Hou et al., 2019). Also, it is unclear if the tested cutin aliphatic monomers are the most potent class of cutin-derived DAMPs. Esterase-based degradation of cutin progresses through ester-cleavage, likely releasing cutin oligomers and not only monomers (Beneloujaephajri et al., 2013). This raises the hypothesis that cutin oligomers act as DAMPs, similar to that proposed for cutin monomers.

To investigate the hypothesis that cutin oligomers (COMs) can activate PTI responses, the cutin polymer was first isolated from tomato peel (Moreira et al., 2020; Bento et al., 2021), and subsequently broken down through a mild chemical hydrolysis to generate COMs. The ability of the produced COMs to activate calcium influx, MAPK activation and transcriptional reprograming in *Arabidopsis* was investigated. The results clearly indicate that COMs act as DAMPs. Spectroscopy and spectrometry analyses suggested that the elicitors are dimers and/or trimers consisting mostly of esterified 10,16-dihydroxyhexadecanoic acid units (dihydroxy-C16 acid), one of which possibly methylated. The hypothesis that cutin disruption releases oligomers able to act as DAMPs is discussed in detail.

Results and discussion

Cutin polymer activates a ROS burst in Arabidopsis

We hypothesized that the degradation of the plant polyester cutin is coordinated with the release of polymeric/oligomeric variants capable of eliciting hallmark early plant immune responses. We first tested a cutin polymeric variant ability to induce a ROS burst in *Arabidopsis*. *Arabidopsis* is a well-established model plant for studying PTI due to the diversity of established protocols and plant resources, including characterized mutants and reporter lines (Felix et al., 1999). The ROS burst was measured through a well-established protocol that detects a luminescence signal produced in the presence of H_2O_2 due to peroxidase (here, horseradish peroxidase, HRP)-mediated conversion of luminol (Zhu et al., 2016).

To obtain the cutin, an ionic liquid extractant was applied to isolate a highly pure cutin polymer (hereafter simply referred as cutin), showing minor ester cleavage (Moreira et al., 2020). This method ensures faster and simpler recovery of cutin compared to the conventional enzyme-based isolation (Moreira et al., 2020). Cutin was purified from tomato pomace since its high availability as an agroindustry residue (European Commission, 2021) enables the production of large amounts of polymeric structures. Moreover, previous studies showed that cutin purified with an ionic liquid from tomato pomace (consisting of peels, seeds and stems) is virtually similar to that obtained from the tomato peel fraction alone (Escórcio et al., 2022).

Exposure of seedlings of *Arabidopsis* to cutin (suspension in MiliQ water) resulted in a clear ROS burst (Fig. 1A-B and Supplemental Fig. S1). Flg22, a 22-amino acid peptide derived from bacterial flagellin, is a well-established strong inducer of plant immunity (Felix et al., 1999; Correia et al., 2020) (used here as positive control). The effect was reproducible, and the response was not depleted at 45 min post-treatment (Fig. 1B). On the contrary, pure compounds (commercially available), which are representative of tomato cutin constituents: long chain fatty acids, hydroxycinnamic acids or fatty acid monoglycerides having variable side chains, did not induce a ROS burst under the tested conditions (Fig. 1C, Supplemental Fig. S2). Cutin hydrolysates, which are obtained by an extensive hydrolysis of the cutin, consist almost exclusively of aliphatic monomers with a few aromatic monomers (Escórcio et al., 2022). These hydrolysates also did not elicit a ROS burst (Fig. 1D). Collectively, the results suggest that once the polymeric backbone of the plant polyester is

deconstructed to its composing monomeric pieces, its capability to elicit a ROS burst is lost; hence some preservation of the polymeric backbone might be required for the eliciting of a ROS burst in *Arabidopsis*.

To test if small chains of monomers linked together through ester linkages; *i.e*. oligomers (<7), could act as elicitors, we prepared cutin oligomeric mixtures (COMs). To produce these, cutin was depolymerized through a mild chemical hydrolysis and the released molecules were collected (*see Materials and Methods*). The produced COMs were unable to trigger a ROS burst (Fig. 1E). However, no effect was detected when the seedings were co-treated with flg22 and COM, although flg22 alone clearly induced a ROS burst (Fig. 1F). This result suggests that constituents of the COM preparation interfered with the reporter of luminescence. In fact, the COM contains phenolic compounds (Supplemental, Table S1) and phenol oxidation has been reported to inactivate HRP activity in a concentration dependent mode (*i.e.* ratio enzyme:inhibitor) (Mao et al., 2013). Cutin hydrolysates (mixture of all hydrolysable cutin monomers) also contain low levels of phenolic compounds (Escórcio et al., 2022). There are alternative methods for ROS measurement; for example, DAB staining has been used to detect the accumulation of intracellular ROS in response to treatment with cutin aliphatic monomers, specifically hydroxy palmitic acid (HPA) (Kim et al., 2008; Park et al., 2008). Thus, while we observed that cutin aliphatic monomers did not induce an apoplastic ROS burst using a luminol-based assay, we cannot disregard the possibility that accumulation of intracellular ROS might occur at extended post-treatment periods.

The results show that treatment of *Arabidopsis* with cutin induced a ROS burst (Fig. 1A) but not any of the tested pure cutin constituents (Fig. 1C). Due to the aforementioned technical limitation, to further test COMs activity as potential elicitors of plant immunity, we converged towards the calcium response - another hallmark early immune response.

Cutin and COMs, but not cutin hydrolysates, activate a calcium influx in Arabidopsis

Both cutin and COMs showed a clear and reproducible induction of calcium influx in *Arabidopsis* plants expressing aequorin (Fig. 2A, 2B), a widely used

calcium activated reporter of immune responses in plants (Mithöfer and Mazars, 2002). The response patterns were however different: cutin response was bimodal with maximum values at 3 min and 12 min (Fig. 2A), whereas COM response was monomodal with a maximum between 3 and 5 min (Fig. 2B). This result suggests that cutin may comprise several classes of chemical elicitors, one of which is prevalent in the COM fraction. *Nicotiana benthamiana* plants expressing aequorin (Segonzac et al., 2011) when exposed to COMs also showed a calcium influx having a monomodal response-type (Supplemental Fig. S3A). Since the eliciting molecules were similarly recognized by both tested plants, the elicitors are likely not species-specific.

Finally, no induction of a calcium influx was observed upon treatment of *Arabidopsis* seedlings with either HPA or cutin hydrolysates increasing concentrations (Supplemental Fig. S3B-C). Collectively, these data validate the opening hypothesis that cutin small oligomers may act as elicitors of PTI. Mild deconstruction of the polymer potentiates its capability to induce a calcium influx in *Arabidopsis,* but its complete depolymerization abolished this eliciting effect.

Cutin oligomers trigger MAPK activation in Arabidopsis

PTI signaling events occurring downstream to elicitor perception involve the activation of MAP kinases (Yu et al., 2017; DeFalco and Zipfel, 2021). Accordingly, the capabilities of COM to activate MAP kinases in *Arabidopsis* Col-0 seedlings was evaluated. This immunoblot-based assay allows the detection of the phosphorylated (active) forms of MAPK 3, 4, 6 and 11 during PTI signaling (Willmann et al., 2014). Short (10 min) exposure of *Arabidopsis* seedlings to COM activated hallmark MAPK activation; similar to that observed when the plants were exposed to flg22 (Fig. 3). In addition to the wild type plants, three mutants were also tested, single: *cerk1-2* (Ranf et al., 2011), double: *bak1-5 bkk1* (Roux et al., 2011), and triple: *bak1-5 bbk1 cerk1* (*bbc*) (Xin et al., 2016). CHITIN ELICITOR RECEPTOR KINASE 1 (CERK1) is a common co-receptor for LysM-type PRRs (Macho and Zipfel, 2014) while BRASSINOSTEROID INSENSITIVE 1-ASSOCIATED KINASE 1 (BAK1) and BAK1-LIKE KINASE 1 (BKK1) are common co-receptors for leucine-rich repeat-type PRRs (Tang et al., 2017). Thus, differences in the response pattern of the

selected mutants may reveal potential families of PRR(s) that recognize the elicitor(s) within COM. The results showed that COM induced a clear activation of MAP kinases in all the mutants tested, similar to that observed in the wild-type plants (Fig. 3). The observation that MAPK activation was similar in all mutants is suggestive of a perception mechanism independent on the families of PRRs known to associate with CERK1 and SERKs. Ultimately, these results suggest that COMs triggered a MAPK-mediated signaling cascade, opening the hypothesis that COM exposure also involves transcriptional reprogramming.

Cutin oligomers treatment induced a transcriptional reprograming consistent with activation of PTI

We evaluated the transcriptional reprogramming in *Arabidopsis* seedlings upon a 30-min treatment with COM compared to mock control (RNA-seq). Previous studies covering distinct PTI elicitors showed significant responses at 30 min post-treatment (Bjornson et al., 2021). Principal components analysis (PCA) demonstrates that their transcriptomic profiles are clearly separating from each other (Supplemental Fig. S4). A total of 528 differentially expressed genes (DEGs) resulted from the COM treatment, of which 479 genes were upregulated, while only 49 were downregulated compared to the mock treatment (Fig. 4A). Enriched gene ontology (GO) categories were only obtained for the subset of upregulated genes due to the small number of downregulated genes. An enrichment for terms related to activation of plant immunity, particularly ‘response to wounding’ and ‘response to other organism’ was noticed (Fig. 4B).

The observed transcriptional reprogramming induced by the COM treatment was compared to that induced (*i.e.* upregulated) by seven other well-characterized elicitors of plant immunity, recently reported by Bjornson *et al.* (Bjornson et al., 2021). The COM effect presents similarity with that of the other elicitors: 140 induced genes (~30%) responded to COM and the other PTI elicitors (Fig. 4C). The transcriptional reprogramming induced by COM has however some uniqueness since 105 induced genes (~20%) were not induced by any of the other tested elicitors (Fig. 4C). In fact, such level of specificity in transcriptional reprogramming was previously only observed for flg22 (Bjornson et al., 2021) (Fig. 4C). The lower number of induced genes by COM treatment

could be related to the single time point used, differently from the other elicitors of PTI where multiple timepoints were used. The genes induced only by COM (and not by the other elicitors) were compared with genes found to be upregulated under abiotic stress (seven types of stresses were considered, *see Materials and Methods*). We observed that among these, 32 genes were induced solely by COM and not by any of the abiotic stresses (Supplemental Table S2 and Table S3); further suggestive of a certain degree of uniqueness on the COM's effect.

The uniqueness of the COM treatment was further demonstrated through a correlation analysis of all elicitor transcriptomic datasets at the 30-min timepoint (Fig. 4D). At this timepoint, COM effect is not well correlated with any of the other tested elicitors; for example, bacterial hydroxy-fatty acid (3-OH-FA) and fungal chitooctamer (CO8). It also showed no correlation with the effect of oligogalacturonides (OGs) originating from plant cell wall pectin degradation. Cutin anchoring to the cell wall is a long-standing debate, but the involvement of polysaccharide-based moieties has been suggested (Philippe et al., 2020b). Polysaccharides can be found at very low amounts in cutin isolated using the ionic liquid extractant (Bento et al., 2021), but it remains an unresolved question if the detected polysaccharide-moieties are covalently linked to cutin. No glycoside-type linkages were detected in the NMR spectral fingerprint of a highly concentrated COM sample: 40 mg to allow the detection of low-intensity signals (Supplemental Fig. S5A). Several molecules derived from cell wall polysaccharides can act as elicitors, for example OGs (Ferrari et al., 2013), cellobiose (de Azevedo Souza et al., 2017), arabinoxylan oligosaccharides (Mélida et al., 2020) and mixed-linked β-1,3/1,4-glucans (Rebaque et al., 2021). However, the reported amounts for their eliciting effects (de Azevedo Souza et al., 2017) usually range from $\mu g \cdot mL^{-1}$ to $mg \cdot mL^{-1}$. These levels are higher than those detected in the COM preparations that were observed to contain only picograms of hydrolysable sugars *per* mg of COM (Supplemental Fig. S5B). The acquired data thus indicate that the molecules within the COM preparation acting as elicitors have a lipidic nature.

Guiding principles on the chemistry of COMs that are able to elicit a rapid immune response in Arabidopsis

COM preparations have been shown to consist of oligomers and monomers (Escórcio et al., 2022). During infection, pathogens can secrete enzymes able to hydrolyze ester-type linkages present in cutin (Serrano et al., 2014); breaking the structural integrity of the cutin barrier to allow pathogen invasion of the infected plant tissue. To mimic such progressive attack of cutin, after obtaining a COM preparation, the non-hydrolyzed cutin fraction was recovered. The recovered cutin was subjected to a second round of mild hydrolysis and subsequently processed to obtain a COM II fraction. In *Arabidopsis* plants, the signal-intensity of the COM II induced calcium influx was >2-fold higher than that observed after COM treatment (Supplemental Fig. S6). This observation suggests that COM II might be more enriched in active elicitors compared to COM.

The free monomers were detected (and quantified) by GC-MS analysis, which also differentiates the methylated derivatives formed during the cleavage of esters through the methanolysis reaction (Supplemental, Table S1). The presence of oligomers was directly inferred from the detection of both primary (PAE) and secondary aliphatic esters (SAE) through NMR analyses, specifically in the HSQC spectral fingerprints of either COM preparation (Fig. 5A). The integration of their corresponding ^{1}H NMR signals, relative to an internal standard, was used to infer the relative amount of PAE (*i.e.* linear) and SAE (*i.e.* branched) (Fig. 5B). Both types of esterification have been reported before in the spectral fingerprint of several cutin variants (Moreira et al., 2020; Bento et al., 2021; Escórcio et al., 2022). The estimated relative abundances of methyl esters in COM range from 40 to 70% of the total esters, consistent with the GC-MS data (Supplemental, Table S1). To depolymerize all present oligomers, the COM was subjected to hydrolysis and reanalyzed by GC-MS. Comparison of the resultant monomeric profiles of the COM and the resulting hydrolysate, exposed monomers increasing in abundance after hydrolysis (Supplemental, Table S1). The major aliphatic monomer of cutin, dihydroxy-C16 acid, is likely the major building block of the oligomers, distantly followed by 9,10-epoxy-18-hydroxyoctadecanoic acid, nonanedioic acid and hexadecanedioic acid.

A preliminary LC-MS/MS analysis was performed targeting the exact masses of dihydroxy-C16 acid dimers and trimers, carrying or not one methylation (Supplemental, Table S4A). Pure HPA was used to setup the

method (see *Materials and Methods*). The given outputs (Compound Discovery 3.2) were unsupervised since the software automatically computes the most likely ions/adducts to be generated in negative/positive modes for each given mass (Supplemental, Table S4B). In both COMs, dimers were putatively identified, namely two dihydroxy-C16 acid molecules esterified, methylated or not – DP2 (Fig. 6A-B, Supplemental Fig. S7A-B). A trimer of dihydroxy-C16 acid molecules, carrying or not one methylation, was putatively identified only in COM II – DP3 (Fig. 6C-D, Supplemental Fig. S7C-D). These molecules can be a linear chain, yet one side-branch is possible (Fig. 6E-F). The NMR quantification data suggest that linear esters are in average two- to three-fold more abundant than branched esters (Fig. 5B), accordingly the linear DP3 chain is more likely to exist.

A MALDI-TOF method was developed to screen for the putative presence of oligomers up to octamers species (Supplemental Fig. S8). The MALDI-TOF analyses showed the presence of the most abundant free monomers in COM and COM II, some of which in the methylated form (Supplemental, Table S5). The controls - cutin and COMs hydrolysates - also contain the same non-methylated monomers (Supplemental, Table S5). In the COMs, dimers were identified, namely DP2, methylated or not (Fig. 7A), consistent with the LC-MS/MS. To selectively observe species capable of self-ionization such as aromatics, samples analyzed by MALDI-TOF were also analyzed without addition of ionization matrix (LDI-TOF). On the LDI-TOF spectra, other dimers detected consist of a dihydroxy-C16 acid esterified to coumaric acid without, or with one or two methylations - DP2c (Supplemental Fig. S9). The DP2c methylated molecules were only detected in the COM. The cutin hydrolysate (control) showed the presence of the non-methylated forms of DP2 in MALDI-TOF and DP2c in LDI-TOF (Supplemental, Table S5). NMR analyses of 40 mg of either COM, showed the presence of esterified aromatics only in COM (Supplemental, Fig. S10). Finally, the methylated-DP3 and, its non-methylated form, were identified in COM II (Fig. 7B), regardless of undetected in COM possibly due to lower relative abundance. Collectively the data on the COMs (and cutin hydrolysates) suggest that amongst the identified oligomeric species, the best PTI elicitor candidates are linear dimers or trimers composed of dihydroxy-C16 acid units, one of which possibly methylated.

Conclusions

The plant cell wall barrier is an important interface during plant–microbe interactions, where cutin is the outermost polymeric component. Plants are able to recognize damages caused by pathogens, and elicit immune responses for example upon recognition of cell wall-derived fragments acting as DAMPs. As such, the cell wall barrier orchestrates key responses of the plant interaction with the surrounding environment. This rationale has defined the major hypothesis of our study, namely that cutin oligomers act as DAMPs able to trigger plant immune responses. In *Arabidopsis*, cutin oligomers (COMs), obtained through methanolysis of tomato pomace cutin, elicited several hallmark immune responses, including calcium influx (Fig. 2) and MAPK activation (Fig. 3), and a transcriptional response comprising features similar to those activated by well-characterized elicitors (Fig. 4). The perception mechanism of the COMs, which was observed to be independent of BAK1/BKK1 and CERK1 co-receptors, remains yet unresolved.

Chemical analyses identified that the COMs contain trimers and dimers (Fig. 6-7). The strongest elicitor candidates are the dihydroxy-C16 acid dimers (DP2) or trimers (DP3) carrying a methylation. DP2, methylated or not, were detected in both COMs. On the contrary, the DP3 and DP2c (dihydroxy-C16 acid esterified to coumaric acid), carrying or not methylation, were only detected in COM II and COM, respectively. The non-methylated DP2 and DP2c were present in cutin hydrolysates unable to elicit a calcium burst, though the threshold for PTI activation remains unknown. The methylation increases the oligomer's lipophilicity, possibly favoring its diffusion; a hypothesis that requires focused analysis. Methyl-esters are, for example, present in seeds (Annarao et al., 2008) and vegetable oil (di Pietro et al., 2020). However, the isolated cutin polymer, which is deprived of methyl-esters, elicited a rapid ROS burst (Fig. 1A-B) and calcium influx (Fig. 2A). This observation questions the requirement of methylation for immune activation. Fungal lipases can generate methyl esters, for example from vegetable oil (Li et al., 2007). In plants, the modification of cutin degradation products by microbial methyl-transferases remains unknown in the context of PTI. However, methylation to potentiate the eliciting effect of

cutin oligomers, may inspire alternative biotechnological valorization paths for fruit pomaces.

Both the cutin polymer (with minor degree of structural damage) and the generated oligomers acted as PTI elicitors. Previous work by others showed that some cutin monomers also activated some aspects of plant immunity (Kauss et al., 1999; Kim et al., 2008; Park et al., 2008). A step-by-step activation of specific elements of plant immunity by cutin having distinct degrees of structural damage, constitutes an appealing concept that deserves further investigation. The release of oligomeric elicitors during plant infection requires validation to attain a mechanistic understanding of cutin's multiple functions in plant-pathogen interactions. The identity of the precise COM elicitors remain putative, and efficient syntheses are needed to obtain pure compounds. However, COMs clearly constitute a new class of DAMPs. Hence, their production from agro-industrial residues constitutes a promising value chain and may support development of sustainable agricultural bio-based treatments to increase disease resistance.

Materials and Methods

Plant Growth Conditions *Arabidopsis thaliana* Col-0 seeds were germinated on soil and plants were grown for four-weeks in an Aralab Fitoclima climate chamber with 150 $\mu mol \cdot s^{-1} \cdot m^{-2}$ light intensity, following a 10 h/14 h day/night cycle, under constant temperature of 20 °C and 60 % humidity. Plants were watered automatically for 10 min three times *per* week. *Arabidopsis thaliana* Col-0 and the mutants *bak1-5 bkk1*, *cerk1-2*^{AEQ} and *bbc* (Ranf et al., 2011; Roux et al., 2011; Xin et al., 2016), all in the Col-0 background, seeds were germinated on plates with 0.5 x Murashige and Skoog (MS) basal salt mixture supplemented with 1 % (w/v) sucrose and 0.9 % (w/v) phytoagar. After four days, seedlings were transferred to 24-well sterile culture plates containing 0.5x MS mixture supplemented with 1 % (w/v) sucrose and grown in sterile conditions in a Aralab Fitoclima climate chamber with 120 $\mu mol \cdot s^{-1} \cdot m^{-2}$ light intensity, following a 16 h/8 h day/night cycle, under temperatures of 20 ºC during the day and 18 ºC at night. The growth period was 8-days, 11-days or 14-days depending of the subsequent assays.

Solanum lycopersicum 'Moneymaker' seeds were germinated on soil and plants were grown for four weeks on a Conviron climate chamber with 120 $\mu mol \cdot s^{-1} \cdot m^{-2}$ light intensity, following a 12 h/12 h day/night cycle, under temperatures of 21 ºC during the day and 19 ºC at night and constant humidity of 60 %. Plants were watered manually three times *per* week.

Nicotiana benthamiana plants seeds were germinated on soil and plants grown for four weeks on a greenhouse room with 150 $\mu mol \cdot s^{-1} \cdot m^{-2}$ light intensity, following 16 h/8 h day/night cycle, under constant temperature of 24 ºC. These plants were watered automatically daily for 20 min.

Cutin Extraction. Cutin was extracted from tomato pomace as previously described(Moreira et al., 2020). The tomato pomace was obtained from Sumol + Compal, SA., and dried at 60 °C for one week until constant weight. Dry pomace was then milled using a Retsch ZM200 electric grinder (granulometry 0.5 mm; 10000 rpm) and stored at room temperature until further use**.** In brief, tomato pomace and cholinium hexanoate were mixed (1:10) and incubated for 2 h at 100 °C. The reaction was stopped by the addition of 80 mL of DMSO *per* gram of tomato pomace. The polyester was recovered by filtration using a nylon membrane filter (0.45 µm). Purification was obtained by washing with an excess of deionized water to remove all traces of DMSO. Purified cutin were then freeze dried and stored at room temperature for further use. Suspensions of the purified cutin powder were prepared in MiliQ water for testing purposes.

Cutin Hydrolysis. To obtain a cutin oligomeric mixture (COM), a sodium methoxide-catalyzed methanolysis was performed by mixing 0.5 g of cutin with 20 mL of a solution of sodium methoxide(0.1M) in anhydrous methanol, at 40 ºC for 2 h without stirring. At the end of the reaction, the mixture was cooled to room temperature and centrifuged (4 ºC, 30 min, 4000 *g*) to recover the non-hydrolyzed cutin fraction. The supernatant (hydrolyzed fraction) was acidified to pH 3–3.5 by addition of HCl 37 % and subsequently centrifuged (4 °C, 30 min, 4000 *g*). The resulting precipitate was recovered, and the supernatant extracted three times by dichloromethane/water partition to release the hydrolysates; and sodium sulphate anhydrous was added to remove traces of water. The solution was concentrated under a constant nitrogen flux at 40 ºC. To obtain cutin or

COM hydrolysates, a sodium hydroxide alkaline hydrolysis was performed by mixing a solution of 0.5 M NaOH in methanol/water (1:1, v/v) at 95 ºC with the cutin/COM powder, for 4 h. At the end of the reaction, the mixture was cooled to room temperature, then acidified to pH 3/3.5 with 1 M HCl, and subsequently extracted by dichloromethane/water partition to release the hydrolysable constituents. The solution was concentrated under a constant nitrogen flux at 40 ºC.

Immune assays. Leaf discs (collected using a 4-mm biopsy punch) or seedlings were transferred to white 96-well plates (one leaf disc or seedling *per* well) and equilibrated overnight in sterile ultrapure water (ROS measurements) or coelenterazine solution (Calcium measurements). The following day, the equilibration solution was removed, and replaced with a solution containing 100 $\mu g.mL^{-1}$ up to 2 $mg.mL^{-1}$ of COM, cutin hydrolysate, hydroxy palmitic acid (HPA) or cutin (Calcium measurements), and mixed with 1 mM luminol, and 10 $\mu g.mL^{-1}$ HRP in the case of ROS measurements. Positive controls were also prepared with 100 nM (flg22 and Pep1) in MiliQ water, as well as blanks with 0.5 % (v/v) DMSO in MiliQ water or MiliQ water. Luminescence was detected and measured for 30 - 45 min using a Photek system equipped with a photon counting camera (leaf discs) or a Tecan Spark microplate reader (seedlings).

MAPK activation – For MAPK activation assays 14-day-old seedlings were used. The growth media was removed by inverting the plate on clean paper towels. Seedlings were treated for 10 min with 1 mL of 3 $mg{\cdot}mL^{-1}$ of COM, 100 nM flg22 (positive control) or the corresponding mock solutions (solvent control). Two seedlings *per* treatment were dried on clean paper towels, subsequently transferred to 1.5-mL tubes and instantly frozen in liquid nitrogen. All treated seedlings were stored at -80 °C until further use. Frozen seedlings were pulverized using a nitrogen-cooled plastic micro pestle, then mixed with 150 µL of extraction buffer containing 50 mM Tris-HCl pH 7.5, 150 mM NaCl, 2 mM EDTA, 10 %(v/v) glycerol, 2 mM DTT, 1 %(v/v) Igepal, and supplemented with protease and phosphatase inhibitors (equivalent to Sigma-Aldrich plant protease inhibitor cocktail and phosphatase inhibitor cocktails #2 and #3) was added. The tissue was then ground at 1800 rpm using an automatic stirrer

fitted with a plastic micro pestle. The tubes were centrifuged at 15,000 *g* for 20 min at 4 °C in a refrigerated microcentrifuge. After centrifugation, 50 µL of extract were transferred to a fresh 1.5-mL Eppendorf tube. Samples were prepared for SDS-PAGE by heating at 80 °C for 10 min in the presence of 6x SDS loading buffer and 100 mM DTT.

Proteins were loaded to a 12 % (v/v) polyacrylamide gels, separated at 120 V for ≅ 120 min and subsequently transferred to a PVDF membrane at 100 V for 90 min at 4 °C. Membranes were then blocked for 2 h at room temperature or overnight at 4 °C in 5 % (w/v) milk in Tris buffered saline (50 mM Tris-HCl pH 7.4, 150 mM NaCl; TBS) containing 0.1 %(v/v) Tween-20 (TBS-T). Blots were probed in a 1:4000 dilution of the NEB anti-p42/p44-erk primary antibody in 5 % BSA in TBS-T for 2 h, followed by washing 4 times for 10 min each in TBS-T. Blots were then probed with a 1:10000 dilution of anti-rabbit secondary antibody in 5 % milk in TBS-T for 1 h, followed by washing 3 times for 5 min each in TBS-T. Finally, blots were washed for 5 min in TBS and treated with either standard ECL substrate or SuperSignal West Femto high sensitivity substrate (ThermoFisher Scientific). Blots were imaged using a Bio-Rad ChemiDoc Imaging System (Bio-Rad Laboratories).

RNA Extraction and Sequencing. For RNA-seq experiments, 14-day-old seedlings were grown as described above. After nine days of growth in liquid MS medium supplemented with 1 % sucrose, the medium was removed from the wells and replaced with 600 µL of fresh liquid MS per well. The following day, 400 µl of 3 mg/mL of COM in 0.5 % DMSO in MiliQ water or the corresponding mock solution were added to each well. Seedlings were treated for 30 min and then two were collected and instantly frozen in liquid nitrogen. In total, four biological replicates were generated for each treatment (COM and mock) and stored at -80 ºC for further processing.

Frozen seedlings were pulverized while frozen using a Spex SamplePrep Geno Grinder 2010 at 1500 rpm for 90 s. Total RNA was extracted at 4 ºC from two ground seedlings as previously described(Shi and Bressan, 2006) by addition of 900 µL of TRI reagent (Ambion) and 200 µL of chloroform, recovery of 400 µL from the aqueous phase, precipitation with 500

µL of isopropanol and washing with 70 % ethanol. All samples were then solubilized in 30 µL of RNase-free water. Samples were subsequently subjected to DNase treatment using a TURBO DNA-free Kit (Ambion) according to manufacturer's instructions. The reaction mix was incubated at 37 ºC for 30 min, after which the inactivation reagent was added and incubated for 5 min at room temperature. After centrifugation the supernatant was transferred to a new tube. Quantification and quality assessment of all RNA samples were evaluated on a TapeStation (Agilent) and RNA sequencing performed by the Beijing Genomics Institute (BGI).

RNA-seq data processing. For paired-end RNA sequencing (RNA-seq), libraries were generated at BGI according to the DNBSEQ stranded mRNA library system. Eight samples were indexed and sequenced using the DNBseq™ sequencing platform (20 million reads per sample). Generated FastQ files were analyzed with FastQC, and any low-quality reads were trimmed with Trimmomatic (Bolger et al., 2014).

All libraries were aligned to the *A. thaliana* genome assembly TAIR10 with gene annotations from Ensembl Plants v.49 using the HISAT2 v.2.1.0 pipeline(Kim et al., 2015) followed by read counts with HTSeq v. 0.13.5(Anders et al., 2015). All RNA-seq experiments were carried out with four biological replicates. Differential expression analysis, and quality control principal-component analysis (PCA) and MA plots were generated using the DESeq2 v.1.30.0 R package(Love et al., 2014). The genes that showed |log2| > 1-fold changes in expression with an adjusted P value below 0.05 are defined as significantly differentially expressed genes (DEGs) in this analysis. Transcript abundance was defined as transcripts per kilobase million (TPM). Gene Ontology enrichment of the differentially expressed genes was performed with the topGO v.2.42.0 R package, using the Fisher exact test to attain significantly enriched categories.

Comparative analysis of transcriptome modification upon elicitor treatment. Differentially expressed gene lists in response to seven elicitors (3-OH-FA, CO8, elf18, flg22, nlp20, OGs, Pep1) upon treatment under similar conditions as COM were obtained from Bjornson, *et al*. (2021) (Bjornson et al.,

2021). This study followed a time course from 5 min to 3 h post-elicitation: a gene list was obtained for each elicitor with genes significantly induced at any time. Abiotic stress treatment analysis for seven abiotic stresses (heat, cold, drought, salt, high osmolarity, UV-B light, wounding) was also obtained from Bjornson, *et al.* (2021), based on ATH1 microarray experiments presented in Killian, *et al*. 2007 (Kilian et al., 2007). This study followed a time course from 5 min to 12 h post-elicitation: a gene list was obtained for each elicitor with genes significantly induced at any time up to 3 h. Comparisons and visualizations among differentially expressed genes were performed in R using the tools of the tidyverse v.1.3.1 package (Wickham et al., 2019). Spearman correlation among $\log_2$ (fold changes) for treatments was calculated using the Hmisc package in R v.4.5-0) and visualized using the corrplot package v.0.89. Annotation data for genes induced specifically by COM was obtained from the *Arabidopsis* information resource (TAIR) via Bioconductor package org.At.tair.db v.3.10.0. The raw data and the processed file are deposited in the ArrayExpress (www.ebi.ac.uk/fg/annotare/edit/16708/), publicly available after curation.

Quantitative analyses of total carbohydrate content. To evaluate the polysaccharide content, each COM sample was subjected to an acid hydrolysis (1 M H_2SO_4 in methanol) for 4h at 90 ºC. The hydrolysable sugars were recovered in the supernatant through centrifugation (18514 *g*, 4 °C, 20 minutes) and the pH was neutralized using 5 M NaOH in water. All samples were dried under a flux of nitrogen at room temperature. Quantification of carbohydrates in the dried hydrolysates was performed using the total carbohydrate assay kit from Sigma-Aldrich according to the manufacturer's instructions. The samples were analyzed in triplicates.

NMR characterization of cutin oligomeric mixtures. NMR spectra of COMs were recorded using an Avance III 800 CRYO (Bruker Biospin, Rheinstetten, Germany). All NMR spectra (^{1}H, ^{1}H-^{1}H COSY, ^{1}H-^{13}C HSQC, ^{1}H-^{13}C HMBC) were acquired in DMSO-d_6 using 5 mm-diameter NMR tubes, at 60 °C as follows: 15 mg of COMs in 400 µL of DMSO-d_6 (in triplicate) or for validation 40 mg of COMs in 400 µL of DMSO-d_6. For quantification purposes, 1.25 mg of benzene (internal standard) was added to each sample. MestReNova, Version

11.04-18998 (Mestrelab Research, S.L.) was used to process the raw data acquired in the Bruker spectrometers.

GC-MS characterization of cutin oligomeric mixtures. To release the hydrolysable constituents, the COMs were treated with a solution of 0.5 M NaOH in methanol:water (1:1 [v/v]) at 95 °C for 4 h. The mixture was cooled to room temperature and acidified to pH 3–3.5 with HCl 1 M, spiked with a known concentration of hexadecane (internal standard), and extracted three times with dichloromethane. Sodium sulphate anhydrous was added to the organic phase to remove water and concentrated under a nitrogen flow. The non-hydrolysable fraction was recovered by filtration (cellulose nitrate filter) and subsequently washed, dried, and weighted (recalcitrance). The COMs samples were also analyzed directly, *i.e.* not subjected to alkaline hydrolysis. The dried samples were derivatized in N,O-bis(trimethylsilyl)trifluoroacetamide containing 1 % (v/v) of trimethylchlorosilane in pyridine (5:1), for 30 min at 90 °C. The derivatives were then analyzed by GC-MS (Agilent: 7820A GC and 5977B quadrupole MS; HP-5MS column) as follows: ramp temperature 80 °C, then 2 $°C \cdot min^{-1}$ to 310 °C for 15 min. The MS scan mode, with source at 230 °C and electron impact ionization (EI+, 70 eV) was used for all samples. Data acquisition was accomplished by MSD ChemStation (Agilent Technologies); compounds were identified based on the equipment spectral library (Wiley-National Institute of Standards and Technology) and quantified using external standards of the major classes of the aliphatic monomers (heptadecanoic acid, hexadecanedioic acid and pentadecanol). All samples were analyzed in triplicates, each with technical duplicates.

LC-MS/MS characterization of COMs. The LC-MS/MS protocol was adapted from Bhunia R. *et al.* (2018) (Bhunia et al., 2018). The experiments were performed in a Q Exactive Focus™ Hybrid Quadrupole-Orbitrap™ Mass Spectrometer coupled to a Dionex Ultimate 3000 UHPLC. HPA was used as a standard and prepared in isopropanol:methanol:acetonitrile (1:1:1) at a concentration of 200 ng/µL. The samples were prepared in the same way at 1 µg/µL. Separation was achieved in a Waters XBridge column C18 (2.1x150 mm, 3.5 µm particle size, P/N 186003023), using a gradient of increasing

612 percentage of 20 mM ammonium formate in isopropanol (IPA): acetonitrile
613 (ACN) (75:25) (B) and decreasing percentage of ACN:water (60:40) with 20 mM
614 ammonium formate (A). The total method time was 77 min, the flow rate was
615 0.4 $mL \cdot min^{-1}$, and the column was kept at 37 °C. The data was acquired using
616 the Xcalibur software v.4.0.27.19 (Thermo Scientific). The method consisted of
617 several cycles of Full MS scans (R=70000; Scan range=100-1500 m/z) followed
618 by 3 ddMS2 scans (R=17500; NCE 30 V) in positive and negative mode.
619 External calibration was performed using LTQ ESI Positive/Negative Ion
620 Calibration Solution (Thermo Scientific). Generated mass spectra were
621 processed using Compound Discoverer 3.2 (Thermo) for small molecule
622 identification. The search was performed against the mass list with provided
623 molecular formulas (dimers, trimers), as well as mzCloud MS2 database, KEGG
624 and ChEBI MS1 databases. A 3-ppm mass tolerance was used. The minimum
625 peak intensity (MS1) for detection was 10^6. A manual validation of the
626 assignments for the identified oligomers was performed by inspection the MS2
627 fragmentation profiles against the theoretical fragmentation generated on Mass
628 Frontier 8.0 (Thermo). Theoretical chemical structures for the identified
629 oligomers were generated ChemDraw 21.0.0.
630
631 **LDI-TOF and MALDI-TOF analyses of COMs and corresponding**
632 **hydrolysates.** The samples were analyzed by laser desorption/ionization (LDI)-
633 time-of-flight (TOF) MS and by matrix-assisted laser desorption/ionization
634 (MALDI)-time-of-flight (TOF) MS. As control for monomers, total alkaline
635 hydrolysate of cutin was used. As oligomers control, a batch of oligomers (DP1
636 to DP8) were produced (Supplemental Fig. S8) from purified cutin monomers as
637 previously described (Marc et al., 2021) with small modification. The
638 polymerization time was reduced to 8 h and the oligomers were extracted from
639 the polymer by hot (70 °C) ethanol extraction.
640 For the LDI-TOF analyses, the samples were deposited on a polished
641 steel MALDI target plate and analyzed without any preparation. For the MALDI-
642 TOF analyses, samples were mixed with the matrix solution composed of DHB
643 (2,5-dihydroxybenzoic acid) 3 $mg \cdot mL^{-1}$ in 75% methanol, with 2.5 mM LiCl, in a
644 1:3 ratio (v/v). The mixture (1 µL) was deposited on a polished steel MALDI
645 target plate. Measurements were performed on a rapifleX MALDI-TOF

spectrometer (Bruker Daltonics, Bremen, Germany) equipped with a Smartbeam 3D laser (355 nm, 10000 Hz) and controlled using the Flex Control 4.0 software package. The mass spectrometer was operated in reflectron mode with positive polarity for MALDI-TOF analyses and in negative polarity for LDI-TOF analyses. Spectra were acquired in the range of 180-5000 m/z. Neither the MALDI-TOF nor the LDI-TOF used in these experiments can observe the signal of the free *p*-coumaric acid.

Acknowledgements

The authors are thankful to Pedro Lamosa (ITQB NOVA) for support with the NMR analyses. Mass spectrometry data were generated by the Mass Spectrometry Unit (UniMS), ITQB/iBET, Oeiras, Portugal. We thank Stefanie Ranf for the gift of *cerk1-2*^{AEQ} seeds. All members of the Silva Pereira and Zipfel labs are also thanked for useful discussions.

Funding

We acknowledge funding from the European Research Council through grant ERC 2014-CoG-647928 and from Fundação para a Ciência e Tecnologia (FCT) by Project MOSTMICRO ITQB (UIDB/04612/2020 and UIDP/04612/2020) and to the PESSOA program (Prpc nº 441.00) to Cristina Silva Pereira, and from the University of Zurich to Cyril Zipfel. The NMR data were acquired at CERMAX, ITQB-NOVA, Oeiras, Portugal with equipment funded by FCT. C.J.S.M. is grateful to Aralab (Portugal) for the PhD contract 06/PlantsLife/2017 and to EMBO for the short-term fellowship (#8003). RE and IM are grateful to FCT funding for the PhD scholarship BD/06435/2021 and for the working contract financed by national funds under norma transitória D.L. n.º 57/2016, respectively.

Authors' contributions

CSP and CZ supervised the project and the interpretation of data; CSP prepared the final version of the manuscript. All authors have made substantial contributions to the acquisition, analysis and interpretation of data and contributed to the drafting of the manuscript: CJSM, AB and RE (cutin and COM preparation); CJSM (all plant experiments); CJSM, MB and CM (RNA seq); AST, CJSM and RE (GC-MS); AB and RE (NMR); IM and CJSM (LC-MS/MS); BB and MF (MALDI-TOF); CJSM (preparation of the initial draft of the manuscript). All authors read and approved the final version of the manuscript.

690

691 ## References

692 **Anders S, Pyl PT, Huber W** (2015) HTSeq—a Python framework to work with high-
693 throughput sequencing data. Bioinformatics **31**: 166–169

694 **Annarao S, Sidhu OP, Roy R, Tuli R, Khetrapal CL** (2008) Lipid profiling of developing
695 Jatropha curcas L. seeds using 1H NMR spectroscopy. Bioresour Technol **99**: 9032–
696 9035

697 **de Azevedo Souza C, Li S, Lin AZ, Boutrot F, Grossmann G, Zipfel C, Somerville SC**
698 (2017) Cellulose-derived oligomers act as damage-associated molecular patterns
699 and trigger defense-like responses. Plant Physiol **173**: 2383–2398

700 **Beneloujaephajri E, Costa A, L'Haridon F, Métraux J-P, Binda M** (2013) Production of
701 reactive oxygen species and wound-induced resistance in Arabidopsis thaliana
702 against Botrytis cinereaare preceded and depend on a burst of calcium. BMC Plant
703 Biology 2013 13:1 **13**: 1–10

704 **Bento A, Moreira CJS, Correia VG, Escórcio R, Rodrigues R, Tomé AS, Geneix N, Petit J,**
705 **Bakan B, Rothan C, et al** (2021) Quantification of Structure-Property Relationships
706 for Plant Polyesters Reveals Suberin and Cutin Idiosyncrasies. ACS Sustain Chem
707 Eng **9**: 15780–15792

708 **Bhunia RK, Showman LJ, Jose A, Nikolau BJ** (2018) Combined use of cutinase and high-
709 resolution mass-spectrometry to query the molecular architecture of cutin. Plant
710 Methods **14**: 1–17

711 **Bjornson M, Pimprikar P, Nürnberger T, Zipfel C** (2021) The transcriptional landscape
712 of Arabidopsis thaliana pattern-triggered immunity. Nat Plants **7**: 579

713 **Bolger AM, Lohse M, Usadel B** (2014) Trimmomatic: a flexible trimmer for Illumina
714 sequence data. Bioinformatics **30**: 2114–2120

715 **Buxdorf K, Rubinsky G, Barda O, Burdman S, Aharoni A, Levy M** (2014) The
716 transcription factor SlSHINE3 modulates defense responses in tomato plants.
717 Plant Mol Biol **84**: 37–47

718 **Correia VG, Bento A, Pais J, Rodrigues R, Haliński P, Frydrych M, Greenhalgh A,**
719 **Stepnowski P, Vollrath F, King AWT, et al** (2020) The molecular structure and
720 multifunctionality of the cryptic plant polymer suberin. Mater Today Bio **5**: 100039

721 **DeFalco TA, Zipfel C** (2021) Molecular mechanisms of early plant pattern-triggered
722 immune signaling. Mol Cell **81**: 3449–3467

723 **Delwiche CF, Cooper ED** (2015) The evolutionary origin of a terrestrial flora. Current
724 Biology **25**: R899–R910

725 **Escórcio R, Bento A, Tomé AS, Correia VG, Rodrigues R, Moreira CJS, Marion D, Bakan**
726 **B, Silva Pereira C** (2022) Finding a Needle in a Haystack: Producing Antimicrobial
727 Cutin-Derived Oligomers from Tomato Pomace. ACS Sustain Chem Eng **10**: 11415–
728 11427

729 **European Commission** (2021) The tomato market in the EU: Vol. 1: Production and area
730 statistics.

731 **Felix G, Duran JD, Volko S, Boller T** (1999) Plants have a sensitive perception system for
732 the most conserved domain of bacterial flagellin. The Plant Journal **18**: 265–276

733 **Ferrari S, Savatin DV, Sicilia F, Gramegna G, Cervone F, de Lorenzo G** (2013)
734 Oligogalacturonides: plant damage-associated molecular patterns and regulators
735 of growth and development. Front Plant Sci **0**: 49

736 **Fich EA, Segerson NA, Rose JKC** (2016) The Plant Polyester Cutin: Biosynthesis,
737 Structure, and Biological Roles. Annu Rev Plant Biol **67**: 207–233

738 **Hou S, Liu Z, Shen H, Wu D** (2019) Damage-Associated Molecular Pattern-Triggered
739 Immunity in Plants. Front Plant Sci. doi: 10.3389/FPLS.2019.00646

740 **Kauss H, Fauth M, Merten A, Jeblick W** (1999) Cucumber hypocotyls respond to cutin
741 monomers via both an inducible and a constitutive H2O2-generating system. Plant
742 Physiol **120**: 1175–1182

743 **Kilian J, Whitehead D, Horak J, Wanke D, Weinl S, Batistic O, D'Angelo C, Bornberg-**
744 **Bauer E, Kudla J, Harter K** (2007) The AtGenExpress global stress expression data
745 set: protocols, evaluation and model data analysis of UV-B light, drought and cold
746 stress responses. The Plant Journal **50**: 347–363

747 **Kim D, Langmead B, Salzberg SL** (2015) HISAT: a fast spliced aligner with low memory
748 requirements. Nature Methods 2015 12:4 **12**: 357–360

749 **Kim TH, Park JH, Kim MC, Cho SH** (2008) Cutin monomer induces expression of the rice
750 OsLTP5 lipid transfer protein gene. J Plant Physiol **165**: 345–349

751 **Kolattukudy PE, Rogers LM, Li D, Hwang CS, Flaishman MA** (1995) Surface signaling in
752 pathogenesis. Proc Natl Acad Sci U S A **92**: 4080–4087

753 **Li W, Du W, Liu D** (2007) Rhizopus oryzae IFO 4697 whole cell-catalyzed methanolysis
754 of crude and acidified rapeseed oils for biodiesel production in tert-butanol
755 system. Process Biochemistry **42**: 1481–1485

756 **Longhi S, Cambillau C** (1999) Structure-activity of cutinase, a small lipolytic enzyme.
757 Biochim Biophys Acta Mol Cell Biol Lipids **1441**: 185–196

758 **Love MI, Huber W, Anders S** (2014) Moderated estimation of fold change and
759 dispersion for RNA-seq data with DESeq2. Genome Biology 2014 15:12 **15**: 1–21

760 **Macho AP, Zipfel C** (2014) Plant PRRs and the activation of innate immune signaling.
761 Mol Cell **54**: 263–272

762 **Mao L, Luo S, Huang Q, Lu J** (2013) Horseradish Peroxidase Inactivation: Heme
763 Destruction and Influence of Polyethylene Glycol. Scientific Reports 2013 3:1 **3**: 1–
764 7

765 **Marc M, Risani R, Desnoes E, Falourd X, Pontoire B, Rodrigues R, Escórcio R, Batista**
766 **AP, Valentin R, Gontard N, et al** (2021) Bioinspired co-polyesters of hydroxy-fatty
767 acids extracted from tomato peel agro-wastes and glycerol with tunable
768 mechanical, thermal and barrier properties. Ind Crops Prod **170**: 113718

Martin LBB, Rose JKC (2014) There's more than one way to skin a fruit: formation and functions of fruit cuticles. J Exp Bot **65**: 4639–4651

Mélida H, Bacete L, Ruprecht C, Rebaque D, del Hierro I, López G, Brunner F, Pfrengle F, Molina A (2020) Arabinoxylan-Oligosaccharides Act as Damage Associated Molecular Patterns in Plants Regulating Disease Resistance. Front Plant Sci **0**: 1210

Mithöfer A, Mazars C (2002) Aequorin-based measurements of intracellular Ca 2+-signatures in plant cells. Biological Procedures Online • **4**: 105–118

Moreira CJS, Bento A, Pais J, Petit J, Escórcio R, Correia VG, Pinheiro Â, Halinski ŁP, Mykhaylyk OO, Rothan C, et al (2020) An ionic liquid extraction that preserves the molecular structure of cutin shown by nuclear magnetic resonance. Plant Physiol. doi: 10.1104/pp.20.01049

Park JH, Suh MC, Kim TH, Kim MC, Cho SH (2008) Expression of glycine-rich protein genes, AtGRP5 and AtGRP23, induced by the cutin monomer 16-hydroxypalmitic acid in Arabidopsis thaliana. Plant Physiology and Biochemistry **46**: 1015–1018

Philippe G, Geneix N, Petit J, Guillon F, Sandt C, Rothan C, Lahaye M, Marion D, Bakan B (2020a) Plant cuticle embedded polysaccharides exhibit specific structural features. New Phytol (in press)

Philippe G, Geneix N, Petit J, Guillon F, Sandt C, Rothan C, Lahaye M, Marion D, Bakan B (2020b) Assembly of tomato fruit cuticles: a cross-talk between the cutin polyester and cell wall polysaccharides. New Phytologist **226**: 809–822

di Pietro ME, Mannu A, Mele A (2020) NMR Determination of Free Fatty Acids in Vegetable Oils. Processes 2020, Vol 8, Page 410 **8**: 410

Ranf S, Eschen-Lippold L, Pecher P, Lee J, Scheel D (2011) Interplay between calcium signalling and early signalling elements during defence responses to microbe- or damage-associated molecular patterns. The Plant Journal **68**: 100–113

Rebaque D, Hierro I del, López G, Bacete L, Vilaplana F, Dallabernardina P, Pfrengle F, Jordá L, Sánchez-Vallet A, Pérez R, et al (2021) Cell wall-derived mixed-linked β-1,3/1,4-glucans trigger immune responses and disease resistance in plants. The Plant Journal **106**: 601–615

Roux M, Schwessinger B, Albrecht C, Chinchilla D, Jones A, Holton N, Malinovsky FG, Tör M, Vries S de, Zipfel C (2011) The Arabidopsis Leucine-Rich Repeat Receptor–Like Kinases BAK1/SERK3 and BKK1/SERK4 Are Required for Innate Immunity to Hemibiotrophic and Biotrophic Pathogens. Plant Cell **23**: 2440

Segonzac C, Feike D, Gimenez-Ibanez S, Hann DR, Zipfel C, Rathjen JP (2011) Hierarchy and Roles of Pathogen-Associated Molecular Pattern-Induced Responses in Nicotiana benthamiana. Plant Physiol **156**: 687

Serrano M, Coluccia F, Torres M, L'Haridon F, Métraux J-P (2014) The cuticle and plant defense to pathogens. Front Plant Sci **0**: 274

Shi H, Bressan R (2006) RNA Extraction. Methods Mol Biol **323**: 345–348

Tang D, Wang G, Zhou J-M (2017) Receptor Kinases in Plant-Pathogen Interactions: More Than Pattern Recognition. Plant Cell **29**: 618–637

Waters ER (2003) Molecular adaptation and the origin of land plants. Mol Phylogenet Evol **29**: 456–463

Wickham H, Averick M, Bryan J, Chang W, McGowan LD, François R, Grolemund G, Hayes A, Henry L, Hester J, et al (2019) Welcome to the Tidyverse. J Open Source Softw **4**: 1686

Willmann R, Haischer DJ, Gust AA (2014) Analysis of MAPK Activities Using MAPK-Specific Antibodies. Methods in Molecular Biology **1171**: 27–37

Xin A, Fry SC (2021) Cutin:xyloglucan transacylase (CXT) activity covalently links cutin to a plant cell-wall polysaccharide. J Plant Physiol **262**: 153446

Xin X-F, Nomura K, Aung K, Velásquez AC, Yao J, Boutrot F, Chang JH, Zipfel C, He SY (2016) Bacteria establish an aqueous living space in plants crucial for virulence. Nature **539**: 524

Yeats TH, Rose JKC (2013) The formation and function of plant cuticles. Plant Physiol **163**: 5–20

Yu X, Feng B, He P, Shan L (2017) From Chaos to Harmony: Responses and Signaling upon Microbial Pattern Recognition. https://doi.org/101146/annurev-phyto-080516-035649 **55**: 109–137

Zhu H, Jia Z, Trush MA, Li YR (2016) A Highly Sensitive Chemiluminometric Assay for Real-Time Detection of Biological Hydrogen Peroxide Formation. React Oxyg Species (Apex) **1**: 216

Zipfel C (2014) Plant pattern-recognition receptors. Trends Immunol **35**: 345–351

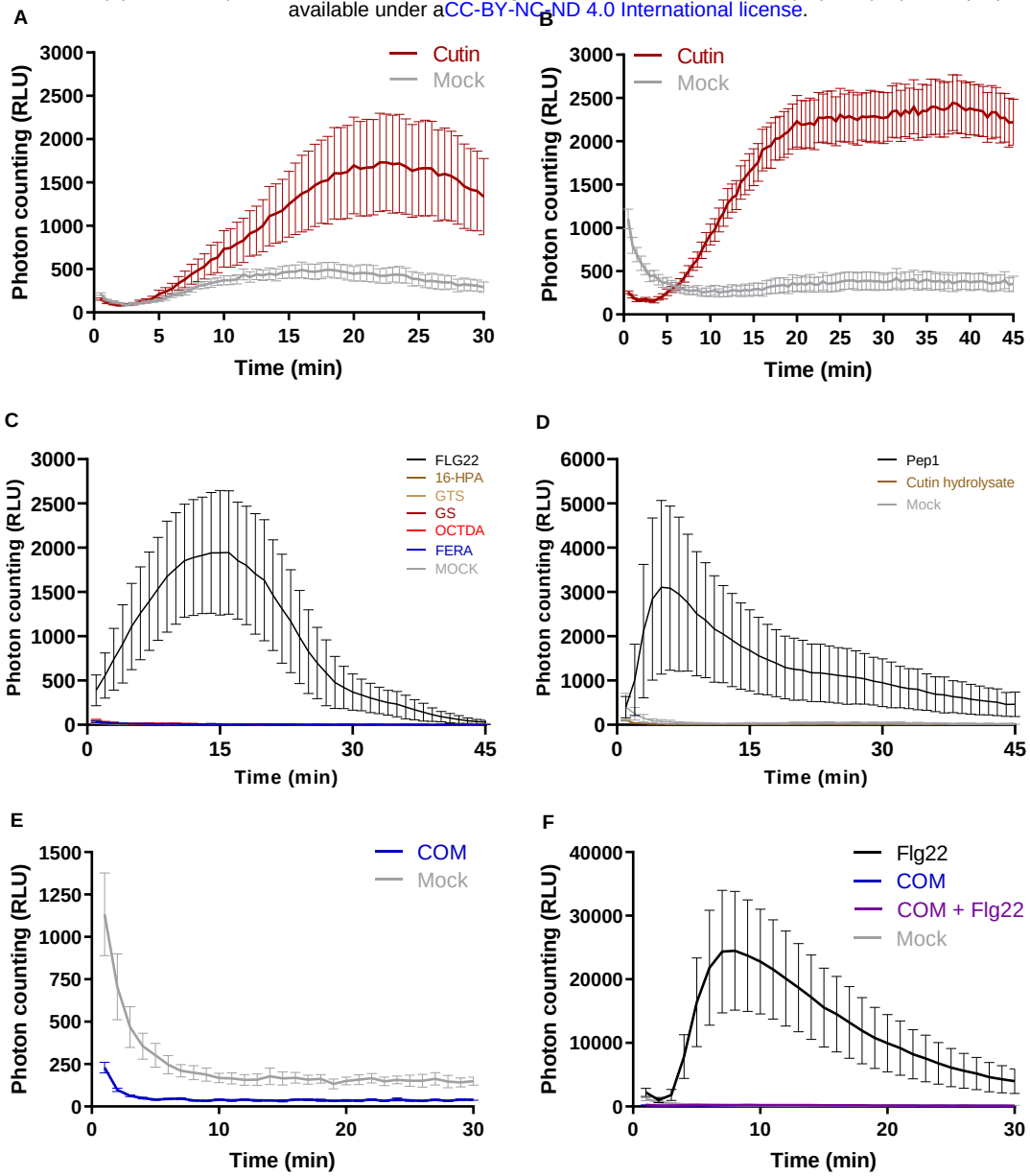

Fig. 1 - Luminescence-based detection of apoplastic ROS in *Arabidopsis thaliana* Col-0 leaf discs upon treatment with 2 mg·mL^{-1} of cutin in MiliQ water for 30 min (**A**) and 45 min (**B**); **C** – 1 mM of commercially available pure monomers (16-hydroxypalmitic acid (16-HPA), octanedioic acid (OCTDA) and ferulic acid (FERA)), and oligomers (glyceryl stearate (GS) and glyceryl tristearate (GTS)), in 10 % ethanol in MiliQ water for 45 min; **D** – 1 mg·ml^{-1} of cutin hydrolysate obtained after alkaline hydrolysis of cutin; **E** – 2 mg·ml^{-1} of COM obtained through the methanolysis of cutin in 0.5 % DMSO in MiliQ water; and **F** – co-treatment with 2 mg·ml^{-1} of COM and 100 nM Flg22 in 0.5 % DMSO in MiliQ water. In all the assays the Mock consists of the solvent. The positive controls were Flg22 (100 nM) or Pep1 (100 nM).

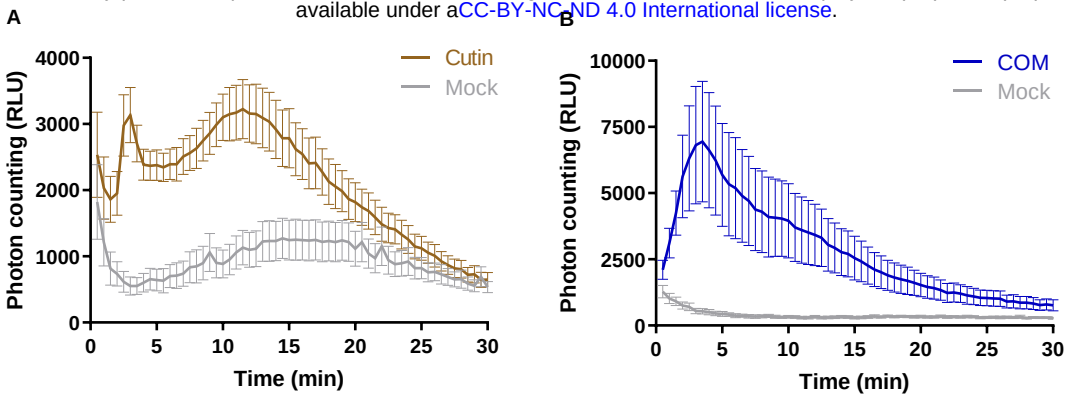

Fig. 2 – Luminescence-based detection of calcium influx in *Arabidopsis thaliana* seedlings expressing the calcium reporter aequorin, upon treatment with: **A** – 1 mg·mL^{1} of cutin in MiliQ water; **B** – 2 mg·mL^{-1} of COM in 0.5 % DMSO in MiliQ water. In all the assays the Mock consists of the solvent.

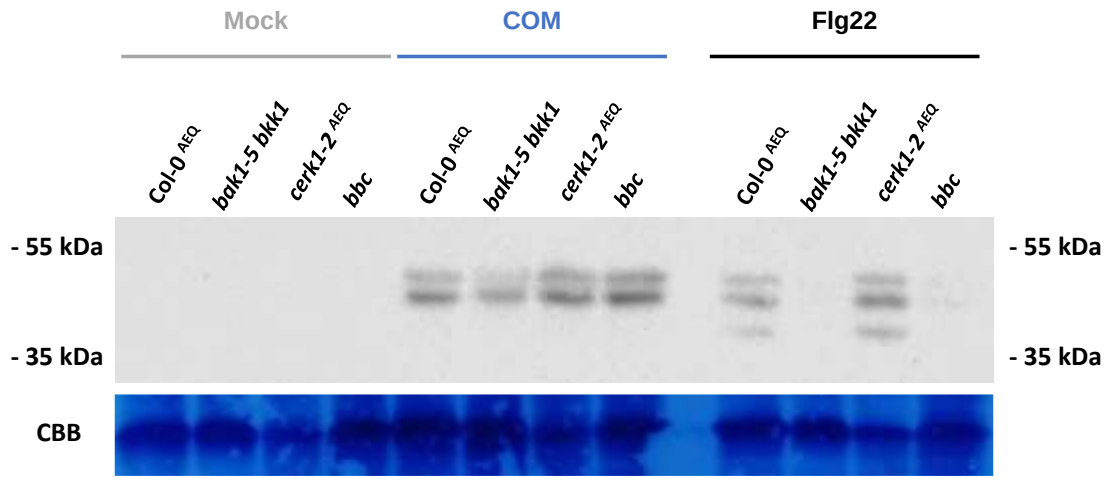

Fig. 3 – Western blot evaluation of MAPK activation in 14-day-old *Arabidopsis thaliana* seedlings from wild type Col-0^{aeq} plants and the *bak1-5 bkk1*, *cerk1-2*^{aeq} *and bbc* mutants, upon treatment with 3 mg·mL^{-1} of COM in 0.5 % DMSO in MiliQ water. The mock consists of the solvent, and the positive control was Flg22 (100 nM, in MiliQ water).

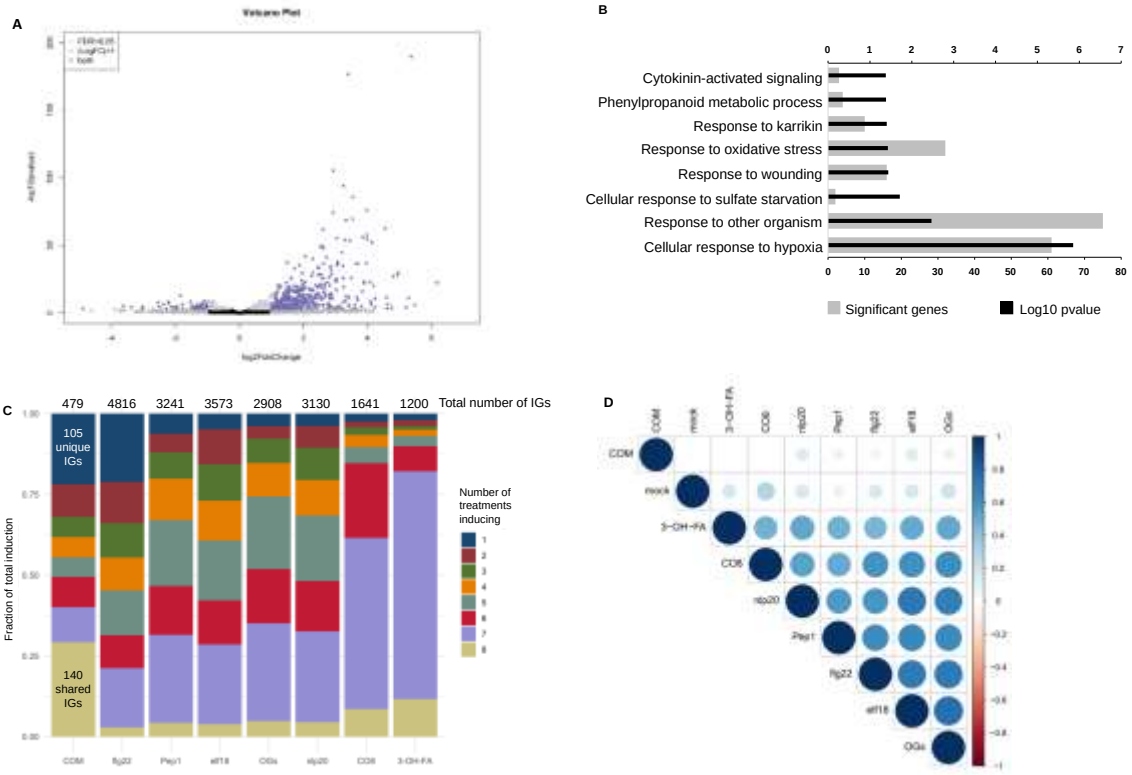

Fig. 4 – (A) Volcano plot representing the statistically significant (adjusted *p*-value < 0.05) differentially expressed genes (Log_2 fold change ≤ -1 or ≥ 1), in *Arabidopsis thaliana* Col-0 plants upon treatment with COM for 30 min (479 upregulated genes and 49 downregulated genes). **(B)** GO term enrichment analysis of the genes that showed upregulation upon treatment with COM for 30 min. **(C)** Comparison of genes induced by treatment of COM with those induced by seven other elicitors of plant triggered immunity. The total number of induced genes (IGs) for each elicitor (over all time points in Bjornson, *et al.* 2021) is presented and the number of genes induced by all treatments or solely by COM are highlighted. **(D)** Correlation plot depicting changes in gene expression between all the elicitors evaluated in the comparative analysis: all transcriptomes compared at 30 min post treatment.

A

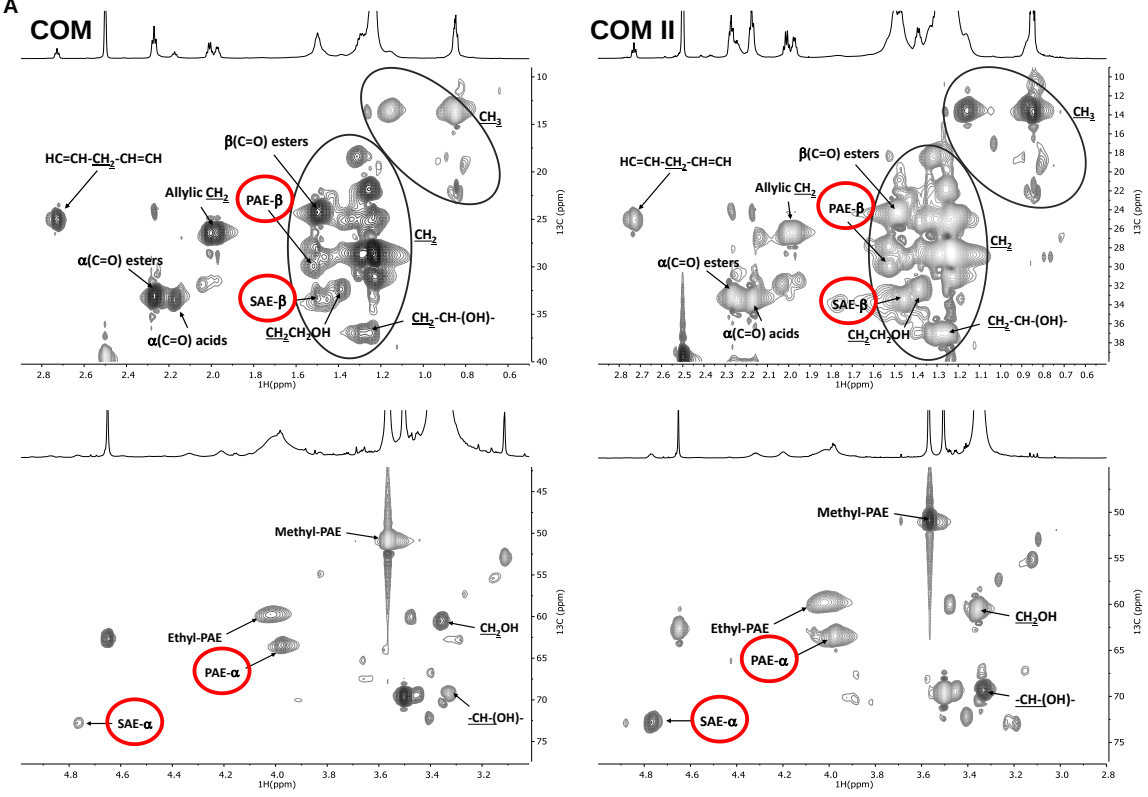

B

	PAE	SAE	ME	EE	ArE	Total Esters
COM	11.16 ± 2.10	3.35 ± 0.33	68.02 ± 4.04	15.85 ± 3.03	1.62 ± 0.20	16.16 ± 2.73
COM II	24.36 ± 2.56	13.62 ± 1.51	40.79 ± 1.62	21.23 ± 1.08	*n.d.*	6.35 ± 1.83

Fig. 5 – (A) NMR characterization of cutin-derived COMs. Magnification of the HSQC spectral regions corresponding to aliphatics for each sample. Some correlations (unlabelled) are uncertain or unidentified. **(B)** NMR quantification of the relative abundances of esters types present in each COM calculated through the integration of signals in the corresponding ^{1}H NMR spectra. Ester types detected on this analysis include, PAE (Primary aliphatic esters), SAE (Secondary aliphatic esters), ME (Methyl esters), EE (Ethyl esters) and ArE (Aromatic Esters). Esters that were not detected on a sample are labelled as *n.d.*

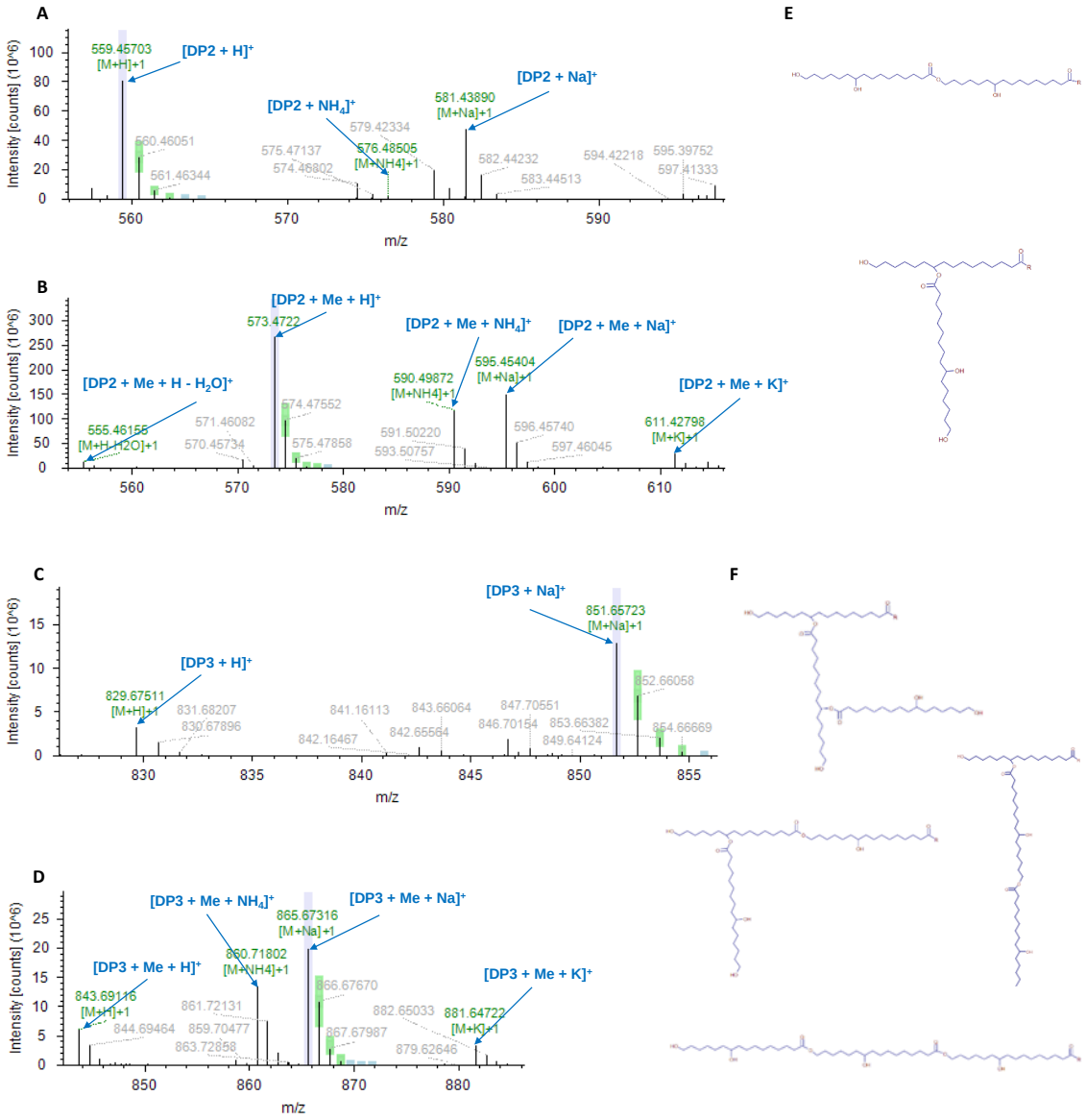

Fig. 6 – LC-MS/MS characterization of COM II (representative spectra for both COMs) in positive mode. MS1 spectra of the detected dimer composed by ester linked molecules of 10,16-dihydroxyhexadecanoic acid (DP2) in the non-methylated (**A**) and methylated (**B**) forms. MS1 spectra of the detected trimer composed by ester linked molecules of 10,16-dihydroxyhexadecanoic acid (DP3) in the non-methylated (**C**) and methylated (**D**) forms. Possible chemical configurations of the putatively identified oligomers (**E-F**), where R corresponds to an OH or CH_3 group for the non-methylated and methylated forms, respectively. Lavender is presented when the labelled centroid matches the monoisotopic mass of the expected compound ion; Green is presented when the labelled centroid matches the delta mass and the relative intensity of the theoretic isotope pattern within the specified tolerances; Blue is presented when

the expected centroid for this *m/z* value might be missing because its theoretic intensity is at the level of the baseline noise. The corresponding MS2 spectra are shown in Supplemental Fig. S7.

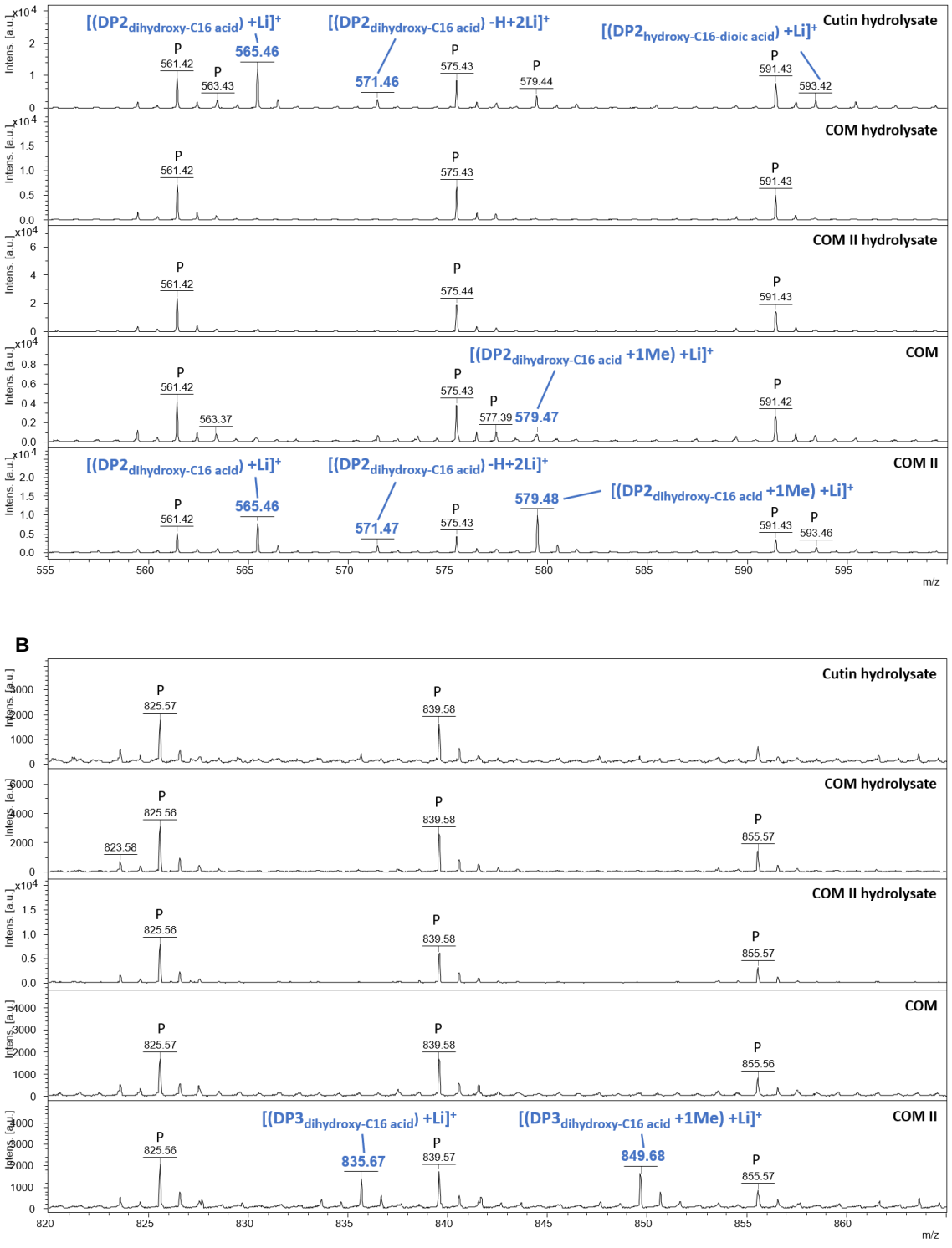

Fig. 7 – MALDI-TOF (+) spectra of cutin hydrolysate, COMs hydrolysates and COMs. The range 555-600 Da corresponds to expected masses for DP2s (**A**). The range 820-865 Da corresponds to expected masses for DP3s (**B**). Annotations were deduced from exact mass measurements. Black star indicates an ion from the MALDI matrix. “p” indicates an ion from PEG contamination.

Parsed Citations

Anders S, Pyl PT, Huber W (2015) HTSeq-a Python framework to work with high-throughput sequencing data. Bioinformatics 31: 166–169
Google Scholar: Author Only Title Only Author and Title

Annarao S, Sidhu OP, Roy R, Tuli R, Khetrapal CL (2008) Lipid profiling of developing Jatropha curcas L. seeds using 1H NMR spectroscopy. Bioresour Technol 99: 9032–9035
Google Scholar: Author Only Title Only Author and Title

de Azevedo Souza C, Li S, Lin AZ, Boutrot F, Grossmann G, Zipfel C, Somerville SC (2017) Cellulose-derived oligomers act as damage-associated molecular patterns and trigger defense-like responses. Plant Physiol 173: 2383–2398
Google Scholar: Author Only Title Only Author and Title

Beneloujaephajri E, Costa A, L'Haridon F, Métraux J-P, Binda M (2013) Production of reactive oxygen species and wound-induced resistance in Arabidopsis thaliana against Botrytis cinereaare preceded and depend on a burst of calcium. BMC Plant Biology 2013 13:1 13: 1–10
Google Scholar: Author Only Title Only Author and Title

Bento A, Moreira CJS, Correia VG, Escórcio R, Rodrigues R, Tomé AS, Geneix N, Petit J, Bakan B, Rothan C, et al (2021) Quantification of Structure-Property Relationships for Plant Polyesters Reveals Suberin and Cutin Idiosyncrasies. ACS Sustain Chem Eng 9: 15780–15792
Google Scholar: Author Only Title Only Author and Title

Bhunia RK, Showman LJ, Jose A, Nikolau BJ (2018) Combined use of cutinase and high-resolution mass-spectrometry to query the molecular architecture of cutin. Plant Methods 14: 1–17
Google Scholar: Author Only Title Only Author and Title

Bjornson M, Pimprikar P, Nürnberger T, Zipfel C (2021) The transcriptional landscape of Arabidopsis thaliana pattern-triggered immunity. Nat Plants 7: 579
Google Scholar: Author Only Title Only Author and Title

Bolger AM, Lohse M, Usadel B (2014) Trimmomatic: a flexible trimmer for Illumina sequence data. Bioinformatics 30: 2114–2120
Google Scholar: Author Only Title Only Author and Title

Buxdorf K, Rubinsky G, Barda O, Burdman S, Aharoni A, Levy M (2014) The transcription factor SlSHINE3 modulates defense responses in tomato plants. Plant Mol Biol 84: 37–47
Google Scholar: Author Only Title Only Author and Title

Correia VG, Bento A, Pais J, Rodrigues R, Haliński P, Frydrych M, Greenhalgh A, Stepnowski P, Vollrath F, King AWT, et al (2020) The molecular structure and multifunctionality of the cryptic plant polymer suberin. Mater Today Bio 5: 100039
Google Scholar: Author Only Title Only Author and Title

DeFalco TA, Zipfel C (2021) Molecular mechanisms of early plant pattern-triggered immune signaling. Mol Cell 81: 3449–3467
Google Scholar: Author Only Title Only Author and Title

Delwiche CF, Cooper ED (2015) The evolutionary origin of a terrestrial flora. Current Biology 25: R899–R910
Google Scholar: Author Only Title Only Author and Title

Escórcio R, Bento A, Tomé AS, Correia VG, Rodrigues R, Moreira CJS, Marion D, Bakan B, Silva Pereira C (2022) Finding a Needle in a Haystack: Producing Antimicrobial Cutin-Derived Oligomers from Tomato Pomace. ACS Sustain Chem Eng 10: 11415–11427
Google Scholar: Author Only Title Only Author and Title

European Commission (2021) The tomato market in the EU: Vol. 1: Production and area statistics.
Google Scholar: Author Only Title Only Author and Title

Felix G, Duran JD, Volko S, Boller T (1999) Plants have a sensitive perception system for the most conserved domain of bacterial flagellin. The Plant Journal 18: 265–276
Google Scholar: Author Only Title Only Author and Title

Ferrari S, Savatin DV, Sicilia F, Gramegna G, Cervone F, de Lorenzo G (2013) Oligogalacturonides: plant damage-associated molecular patterns and regulators of growth and development. Front Plant Sci 0: 49
Google Scholar: Author Only Title Only Author and Title

Fich EA, Segerson NA, Rose JKC (2016) The Plant Polyester Cutin: Biosynthesis, Structure, and Biological Roles. Annu Rev Plant Biol 67: 207–233
Google Scholar: Author Only Title Only Author and Title

Hou S, Liu Z, Shen H, Wu D (2019) Damage-Associated Molecular Pattern-Triggered Immunity in Plants. Front Plant Sci. doi:

10.3389/FPLS.2019.00646
Google Scholar: Author Only Title Only Author and Title

Kauss H, Fauth M, Merten A, Jeblick W (1999) Cucumber hypocotyls respond to cutin monomers via both an inducible and a constitutive H2O2-generating system. Plant Physiol 120: 1175–1182
Google Scholar: Author Only Title Only Author and Title

Kilian J, Whitehead D, Horak J, Wanke D, Weinl S, Batistic O, D'Angelo C, Bornberg-Bauer E, Kudla J, Harter K (2007) The AtGenExpress global stress expression data set: protocols, evaluation and model data analysis of UV-B light, drought and cold stress responses. The Plant Journal 50: 347–363
Google Scholar: Author Only Title Only Author and Title

Kim D, Langmead B, Salzberg SL (2015) HISAT: a fast spliced aligner with low memory requirements. Nature Methods 2015 12:4 12: 357–360
Google Scholar: Author Only Title Only Author and Title

Kim TH, Park JH, Kim MC, Cho SH (2008) Cutin monomer induces expression of the rice OsLTP5 lipid transfer protein gene. J Plant Physiol 165: 345–349
Google Scholar: Author Only Title Only Author and Title

Kolattukudy PE, Rogers LM, Li D, Hwang CS, Flaishman MA (1995) Surface signaling in pathogenesis. Proc Natl Acad Sci U S A 92: 4080–4087
Google Scholar: Author Only Title Only Author and Title

Li W, Du W, Liu D (2007) Rhizopus oryzae IFO 4697 whole cell-catalyzed methanolysis of crude and acidified rapeseed oils for biodiesel production in tert-butanol system. Process Biochemistry 42: 1481–1485
Google Scholar: Author Only Title Only Author and Title

Longhi S, Cambillau C (1999) Structure-activity of cutinase, a small lipolytic enzyme. Biochim Biophys Acta Mol Cell Biol Lipids 1441: 185–196
Google Scholar: Author Only Title Only Author and Title

Love MI, Huber W, Anders S (2014) Moderated estimation of fold change and dispersion for RNA-seq data with DESeq2. Genome Biology 2014 15:12 15: 1–21
Google Scholar: Author Only Title Only Author and Title

Macho AP, Zipfel C (2014) Plant PRRs and the activation of innate immune signaling. Mol Cell 54: 263–272
Google Scholar: Author Only Title Only Author and Title

Mao L, Luo S, Huang Q, Lu J (2013) Horseradish Peroxidase Inactivation: Heme Destruction and Influence of Polyethylene Glycol. Scientific Reports 2013 3:1 3: 1–7
Google Scholar: Author Only Title Only Author and Title

Marc M, Risani R, Desnoes E, Falourd X, Pontoire B, Rodrigues R, Escórcio R, Batista AP, Valentin R, Gontard N, et al (2021) Bioinspired co-polyesters of hydroxy-fatty acids extracted from tomato peel agro-wastes and glycerol with tunable mechanical, thermal and barrier properties. Ind Crops Prod 170: 113718
Google Scholar: Author Only Title Only Author and Title

Martin LBB, Rose JKC (2014) There's more than one way to skin a fruit: formation and functions of fruit cuticles. J Exp Bot 65: 4639–4651
Google Scholar: Author Only Title Only Author and Title

Mélida H, Bacete L, Ruprecht C, Rebaque D, del Hierro I, López G, Brunner F, Pfrengle F, Molina A (2020) Arabinoxylan-Oligosaccharides Act as Damage Associated Molecular Patterns in Plants Regulating Disease Resistance. Front Plant Sci 0: 1210
Google Scholar: Author Only Title Only Author and Title

Mithöfer A, Mazars C (2002) Aequorin-based measurements of intracellular Ca 2+-signatures in plant cells. Biological Procedures Online • 4: 105–118
Google Scholar: Author Only Title Only Author and Title

Moreira CJS, Bento A, Pais J, Petit J, Escórcio R, Correia VG, Pinheiro Â, Halinski ŁP, Mykhaylyk OO, Rothan C, et al (2020) An ionic liquid extraction that preserves the molecular structure of cutin shown by nuclear magnetic resonance. Plant Physiol. doi: 10.1104/pp.20.01049
Google Scholar: Author Only Title Only Author and Title

Park JH, Suh MC, Kim TH, Kim MC, Cho SH (2008) Expression of glycine-rich protein genes, AtGRP5 and AtGRP23, induced by the cutin monomer 16-hydroxypalmitic acid in Arabidopsis thaliana. Plant Physiology and Biochemistry 46: 1015–1018
Google Scholar: Author Only Title Only Author and Title

Philippe G, Geneix N, Petit J, Guillon F, Sandt C, Rothan C, Lahaye M, Marion D, Bakan B (2020a) Plant cuticle embedded

polysaccharides exhibit specific structural features. New Phytol (in press)
Google Scholar: Author Only Title Only Author and Title

Philippe G, Geneix N, Petit J, Guillon F, Sandt C, Rothan C, Lahaye M, Marion D, Bakan B (2020b) Assembly of tomato fruit cuticles: a cross-talk between the cutin polyester and cell wall polysaccharides. New Phytologist 226: 809–822
Google Scholar: Author Only Title Only Author and Title

di Pietro ME, Mannu A, Mele A (2020) NMR Determination of Free Fatty Acids in Vegetable Oils. Processes 2020, Vol 8, Page 410 8: 410
Google Scholar: Author Only Title Only Author and Title

Ranf S, Eschen-Lippold L, Pecher P, Lee J, Scheel D (2011) Interplay between calcium signalling and early signalling elements during defence responses to microbe- or damage-associated molecular patterns. The Plant Journal 68: 100–113
Google Scholar: Author Only Title Only Author and Title

Rebaque D, Hierro I del, López G, Bacete L, Vilaplana F, Dallabernardina P, Pfrengle F, Jordá L, Sánchez-Vallet A, Pérez R, et al (2021) Cell wall-derived mixed-linked β-1,3/1,4-glucans trigger immune responses and disease resistance in plants. The Plant Journal 106: 601–615
Google Scholar: Author Only Title Only Author and Title

Roux M, Schwessinger B, Albrecht C, Chinchilla D, Jones A, Holton N, Malinovsky FG, Tör M, Vries S de, Zipfel C (2011) The Arabidopsis Leucine-Rich Repeat Receptor–Like Kinases BAK1/SERK3 and BKK1/SERK4 Are Required for Innate Immunity to Hemibiotrophic and Biotrophic Pathogens. Plant Cell 23: 2440
Google Scholar: Author Only Title Only Author and Title

Segonzac C, Feike D, Gimenez-Ibanez S, Hann DR, Zipfel C, Rathjen JP (2011) Hierarchy and Roles of Pathogen-Associated Molecular Pattern-Induced Responses in Nicotiana benthamiana. Plant Physiol 156: 687
Google Scholar: Author Only Title Only Author and Title

Serrano M, Coluccia F, Torres M, L'Haridon F, Métraux J-P (2014) The cuticle and plant defense to pathogens. Front Plant Sci 0: 274
Google Scholar: Author Only Title Only Author and Title

Shi H, Bressan R (2006) RNA Extraction. Methods Mol Biol 323: 345–348
Google Scholar: Author Only Title Only Author and Title

Tang D, Wang G, Zhou J-M (2017) Receptor Kinases in Plant-Pathogen Interactions: More Than Pattern Recognition. Plant Cell 29: 618–637
Google Scholar: Author Only Title Only Author and Title

Waters ER (2003) Molecular adaptation and the origin of land plants. Mol Phylogenet Evol 29: 456–463
Google Scholar: Author Only Title Only Author and Title

Wickham H, Averick M, Bryan J, Chang W, McGowan LD, François R, Grolemund G, Hayes A, Henry L, Hester J, et al (2019) Welcome to the Tidyverse. J Open Source Softw 4: 1686
Google Scholar: Author Only Title Only Author and Title

Willmann R, Haischer DJ, Gust AA (2014) Analysis of MAPK Activities Using MAPK-Specific Antibodies. Methods in Molecular Biology 1171: 27–37
Google Scholar: Author Only Title Only Author and Title

Xin A, Fry SC (2021) Cutin:xyloglucan transacylase (CXT) activity covalently links cutin to a plant cell-wall polysaccharide. J Plant Physiol 262: 153446
Google Scholar: Author Only Title Only Author and Title

Xin X-F, Nomura K, Aung K, Velásquez AC, Yao J, Boutrot F, Chang JH, Zipfel C, He SY (2016) Bacteria establish an aqueous living space in plants crucial for virulence. Nature 539: 524
Google Scholar: Author Only Title Only Author and Title

Yeats TH, Rose JKC (2013) The formation and function of plant cuticles. Plant Physiol 163: 5–20
Google Scholar: Author Only Title Only Author and Title

Yu X, Feng B, He P, Shan L (2017) From Chaos to Harmony: Responses and Signaling upon Microbial Pattern Recognition. https://doi.org/101146/annurev-phyto-080516-035649 55: 109–137
Google Scholar: Author Only Title Only Author and Title

Zhu H, Jia Z, Trush MA, Li YR (2016) A Highly Sensitive Chemiluminometric Assay for Real-Time Detection of Biological Hydrogen Peroxide Formation. React Oxyg Species (Apex) 1: 216
Google Scholar: Author Only Title Only Author and Title

Zipfel C (2014) Plant pattern-recognition receptors. Trends Immunol 35: 345–351